Interactions between Colloidal Particles Induced by Polymer Brushes Grafted onto the Substrate

Kang Chen and Yu-qiang Ma*

National Laboratory of Solid State Microstructures, Nanjing University, Nanjing 210093, China

Received: March 17, 2005; In Final Form: July 2, 2005

We investigate the interaction energy between two colloidal particles on or immersed in nonadsorbing polymer brushes grafted onto the substrate as a function of the separation of the particles by the use of a self-consistent-field theory calculation. Depending on the colloidal size and the penetration depth, we demonstrate the existence of a repulsive energy barrier of several k_BT, which can be interpreted by separating the interaction energy into three parts: colloid−polymer interfacial energy, entropic contribution due to "depletion zone" overlap of colloidal particles, and entropic elastic energy of grafted chains by the compression of particles. The existence of a repulsive barrier which is of entirely entropic origin can lead to kinetic stabilization of the mixture rather than depletion flocculation or phase separation. Therefore, the present result may suggest an approach for controlling the self-assembling behavior of colloids for the formation of target structures, by tuning the colloidal interaction on the grafting substrate under appropriate selection of colloidal size, effective gravity (influencing the penetration depth), and brush coverage density.

Assembling colloidal nanoparticles into ordered structures is essential to the fabrication of nanomaterials with high performance in optical, electrical, and mechanical properties.[1−14] Due to the small length scale and interaction energy, the ordered structures normally are realized by the self-assembly of nanoparticles in solution or at an interface for the required motion to reach minimum energy state.[3] The mechanism of such self-assembling behavior greatly relies on the effective interaction between particles mediated by the environment such as solvent, substrate, and external field. The fundamental element is obviously the effective interaction between two individual colloidal nanoparticles as a function of their distance, and the results will be helpful for our understanding of the collective assembling behavior of a large amount of particles. Usually, the interaction between large colloidal particles in a solution of small ones or nonadsorbing polymers is strongly influenced by the entropic excluded-volume (depletion) forces which were first recognized theoretically by Askura and Oosawa (AO).[15] Such an effect can be successfully used to explain phase separation in colloid−colloid and colloid−polymer mixtures.[16] Interestingly, Lin et al.[13] combined entropic depletion and patterned surfaces to study the self-assembly of colloidal spheres on periodically patterned templates. Many theoretical and experimental works have already been performed to examine the entropic depletion interactions between colloidal particles in different suspensions as depletion agents. The evolved systems include colloid−polymer mixtures,[17−20] colloids in DNA solutions[21] or a nematic liquid crystal/rigid rod background,[22−28] confined colloidal systems,[29,30] and binary hard-sphere mixtures.[31−33] In colloid/polymer suspensions, when the distance between sphere surfaces or between the sphere surface and the wall is smaller than the diameter of the polymer coils, there will be an attractive potential which depends strongly on the polymer concentration. The topology of the phase diagram depends on the ratio of the polymer radius of gyration to the

radius of colloidal particles. Usually, in the colloid limit with small polymer to colloid size ratios, depletion interactions can be well described in pairwise form. On the contrary, the protein limit for larger polymer sizes requires the incorporation of many-body contributions.[20] Direct measurement of the depletion of colloids in semidilute DNA solutions has revealed the range of "depletion zones" proportional to the correlation length.[21] Recently, Fredrickson et al.[34] investigated the potential of mean force between two nanoparticles in a symmetric diblock copolymer matrix using self-consistent-field (SCF) theory.

On the other hand, the grafting of polymer chains to surfaces is a widely used method to modify their properties including adhesion, lubrication, and wetting behavior and has many useful applications such as colloidal stabilization, polymeric surfactants, biocompatibility, and drug carriers. SCF theory formulated in bispherical coordinates was developed to study the interaction between surface-grafted spherical assemblies, and the results show hints to the conditions for colloidal stabilization.[35,36] Recently, a polymer-coated surface has become an alternative substrate for the assembly of colloidal nanoparticles and metal nanocrystals because of the "softness" property of interfaces and the nanoscale characteristic length. The entropic elastic energy of such polymer brushes will play an important role in colloidal assembly, since the typical energies of both polymer-chain stretching and colloidal assembly are comparable to thermal energy. For example, the grafted polymer always exerts a repulsive entropic force on incoming particles, and most works have focused on the interaction between polymer brushes and individual incoming particles and how to prevent the adsorption of colloids such as proteins onto surfaces under various grafting densities, chain lengths, and interactions between the chains and surface.[37−43] Some experiments have adopted a polymer-grafted surface to control the assembly of nanoparticles.[6−9] Assemblies of nanoparticles with number density gradients in two and three dimensions are achieved. However, to the best of our knowledge, there have been no systematic theoretical and experimental studies on the interaction energy between two colloidal particles

* To whom correspondence should be addressed. E-mail: myqiang@nju.edu.cn.
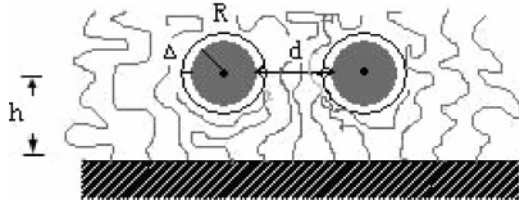
17618 *J. Phys. Chem. B, Vol. 109, No. 37, 2005*

Chen and Ma

Figure 1. Schematic of the two colloidal particles immersed in polymer brushes.

on or immersed in the polymer brushes, which is vitally important to understanding the assembling behavior of many colloidal particles on the polymer-grafted substrate.

In the present paper, we propose a theoretical model to study the effective interaction between two hard colloidal particles on or immersed in polymer brushes with different penetrating depths and the particle radii comparable to the natural size of polymer coils. We try to present a detailed and complete picture on such a unique interaction potential, to understand the kinetic stabilization (i.e., colloidal dispersions) and flocculation of colloids due to the presence of grafting polymer chains. The results are expected to be helpful for assembling experiments of particles on such a substrate with end-grafted polymers.

In our two-dimensional model, the system is placed in the xz plane and the substrate is horizontally fixed at $z = 0$ with n_α uniformly grafted polymer chains (see Figure 1). On the top of the brush is the polymer solvent composed of free chains. Two colloidal particles are modeled by hard circles of radius R located a distance of $d + 2R$ apart and a distance of h from the substrate;[44] there are no attractive or repulsive interactions between them. Each colloidal particle is surrounded by a depletion zone of thickness Δ, where the concentration of polymers becomes depleted compared to that of the bulk solution.[16,21] All polymer chains and colloids are allowed in the region $0 \leq z \leq Z_{max}$. Here, Z_{max} is large enough to avoid the influence of brushes and particles, and as Z approaches Z_{max}, the free "solvent" chains attain their bulk properties.[45] The volume of the system, V, is $L_x \times Z_{max}$, where L_x is the lateral length of the surface along the x axes. The grafting density is defined as $\sigma = n_\alpha/L_x$. All polymer chains are of the same polymerization index N, flexible with the same statistical length a, and incompressible with the segment volume ρ_0^{-1}. The probability distribution for molecular conformations of a Gaussian chain, α, is assumed to take the Wiener form $P[\mathbf{r}_\alpha(s)] \propto \exp[-(3/2a^2)\int_0^1 ds|d\mathbf{r}_\alpha(s)/ds|^2]$, where $\mathbf{r}_\alpha(s)$ denotes the position of segment s on chain α. In every calculation, the positions of two colloids are fixed, and the local volume fraction, $\varphi_p(\mathbf{r})$, of the colloidal particle of radius R with its center at position $\mathbf{r}_c$ is described by taking into account the depletion interaction[46,47] between colloids and polymer chains.

$$\varphi_p(\mathbf{r}) =$$
$$\begin{cases} 1 & |\mathbf{r} - \mathbf{r}_c| \leq R \\ \dfrac{1 + \cos((|\mathbf{r} - \mathbf{r}_c| - R)\pi/\Delta)}{2} & R \leq |\mathbf{r} - \mathbf{r}_c| \leq R + \Delta \\ 0 & R + \Delta \leq |\mathbf{r} - \mathbf{r}_c| \end{cases}$$

We take the incompressibility constraint that $\varphi_\alpha(\mathbf{r}) + \varphi_\beta(\mathbf{r}) + \varphi_p(\mathbf{r}) = 1.0$, which will ensure the exclusion of polymer chains from the depletion zones surrounding the two colloidal particles. Here, $\varphi_\alpha(\mathbf{r})$ and $\varphi_\beta(\mathbf{r})$ represent local volume fractions of grafted and free chains, respectively. The size, Δ, of the depletion zone is determined by depletion agents in the surrounding environment and is independent of the radius, R, of the colloids. For

highly concentrated polymer solutions, the depletion zone thickness is chosen to be about the size of a free segment,[21] and here, we set $\Delta = a$.[48] We define Flory–Huggins interaction parameters between brush and solvent ($\chi_{\alpha\beta}$), brush and particle ($\chi_{\alpha p}$), and solvent and particle ($\chi_{\beta p}$) and take $\chi_{\alpha\beta}N = 0.0$ and $\chi_{\alpha p}N = \chi_{\beta p}N = 20.0$, since we assume that all of the polymers have the same chemical nature, while the colloidal particles are insoluble to polymers. We use the grand canonical form of SCF theory, which has been proven to be powerful in calculating equilibrium morphologies in polymeric systems,[45,46,49-58] to deal with polymer solvents and brushes.

The grand canonical partition function[45] for the system can be written as

$$Z_\mu = \sum_{n_\beta=0}^{\infty} e^{n_\beta N\mu} Z_{n_\alpha, n_\beta} \tag{1}$$

where μ is the chemical potential per segment of solvent chains. Z_{n_α, n_β} is the canonical partition function for n_α grafted chains and n_β free polymers:

$$Z_{n_\alpha, n_\beta} = \frac{1}{n_\alpha!} \frac{1}{n_\beta!} \int \prod_{\alpha=1}^{n_\alpha} D\mathbf{r}_\alpha(s) \, P[\mathbf{r}_\alpha(s)] \prod_{\beta=1}^{n_\beta} D\mathbf{r}_\beta(s) \, P[\mathbf{r}_\beta(s)]$$
$$\delta[1 - \hat{\varphi}_\alpha - \hat{\varphi}_\beta - \varphi_p] \exp\left[-\frac{\nu}{k_B T}\right] \prod_{\alpha=1}^{n_\alpha} \delta(\mathbf{r}_z^\alpha(0)) \tag{2}$$

where the first δ function enforces incompressibility and the second ensures the anchoring of the chain ends on the substrate. k_B is the Boltzmann constant, T is the temperature, and ν is the interaction energy. $\hat{\varphi}_\alpha$ and $\hat{\varphi}_\beta$ are corresponding operators to local concentration φ_α and φ_β. The ends of the brush chains can move on the substrates, although the total number of chains on the surfaces is fixed (we take $\sigma = 0.25$). This is so-called liquid brushes, contrary to solid brushes where the immobile chains are anchored onto surfaces.[40] Here, we consider the liquid brush case because of its wide-ranging applications in colloidal self-assembly and biological organization including cell adhesion and interactions between polymer-coated membranes and proteins (or cells).[40] The SCF theory gives the free energy

$$\frac{NF}{\rho_0 k_B T V} = -\phi \ln\left(\frac{Q_\alpha}{\phi V}\right) - \frac{N}{\rho_0 V} e^{N\mu} Q_\beta + \frac{N\nu}{\rho_0 k_B T V} -$$
$$\frac{1}{V}\int d\mathbf{r}[\xi(1 - \varphi_\alpha - \varphi_\beta - \varphi_p) + w_\alpha \varphi_\alpha + w_\beta \varphi_\beta] \tag{3}$$

where ϕ is the overall volume fraction of brushes. $Q_\alpha = \int d\mathbf{r} \, q_\alpha(\mathbf{r},s) \, q_\alpha^\dagger(\mathbf{r},s)$ represents the single chain partition function of grafted chains subject to the field w_α, and $Q_\beta = \int d\mathbf{r} \, q_\beta(\mathbf{r},s) \, q_\beta(\mathbf{r},1 - s)$ is the partition function for solvent under the field w_β. The end-segment distribution functions $q_i(\mathbf{r},s)$ and $q_i^\dagger(\mathbf{r},s)$ (or $q_i(\mathbf{r},1 - s)$) stand for the probability of finding the sth segment at position $\mathbf{r}$ respectively from two ends of grafted (or free) chains. q_i satisfies the modified diffusion equation $\partial q_i/\partial s = (Na^2/6)\nabla^2 q_i - w_i(\mathbf{r})q_i$. $q_i^\dagger$ meets the same diffusion equation but with the right-hand side multiplied by -1. The interaction, ν, is given by

$$\frac{N\nu}{\rho_0 k_B T V} = \frac{1}{V}\int d\mathbf{r}[\chi_{\alpha\beta}N\varphi_\alpha\varphi_\beta + \chi_{\alpha p}N\varphi_\alpha\varphi_p + \chi_{\beta p}N\varphi_\beta\varphi_p] \tag{4}$$

In SCF theory, the fields and densities are determined by locating saddle points in the free energy expression eq 3. The

Interactions between Colloidal Particles

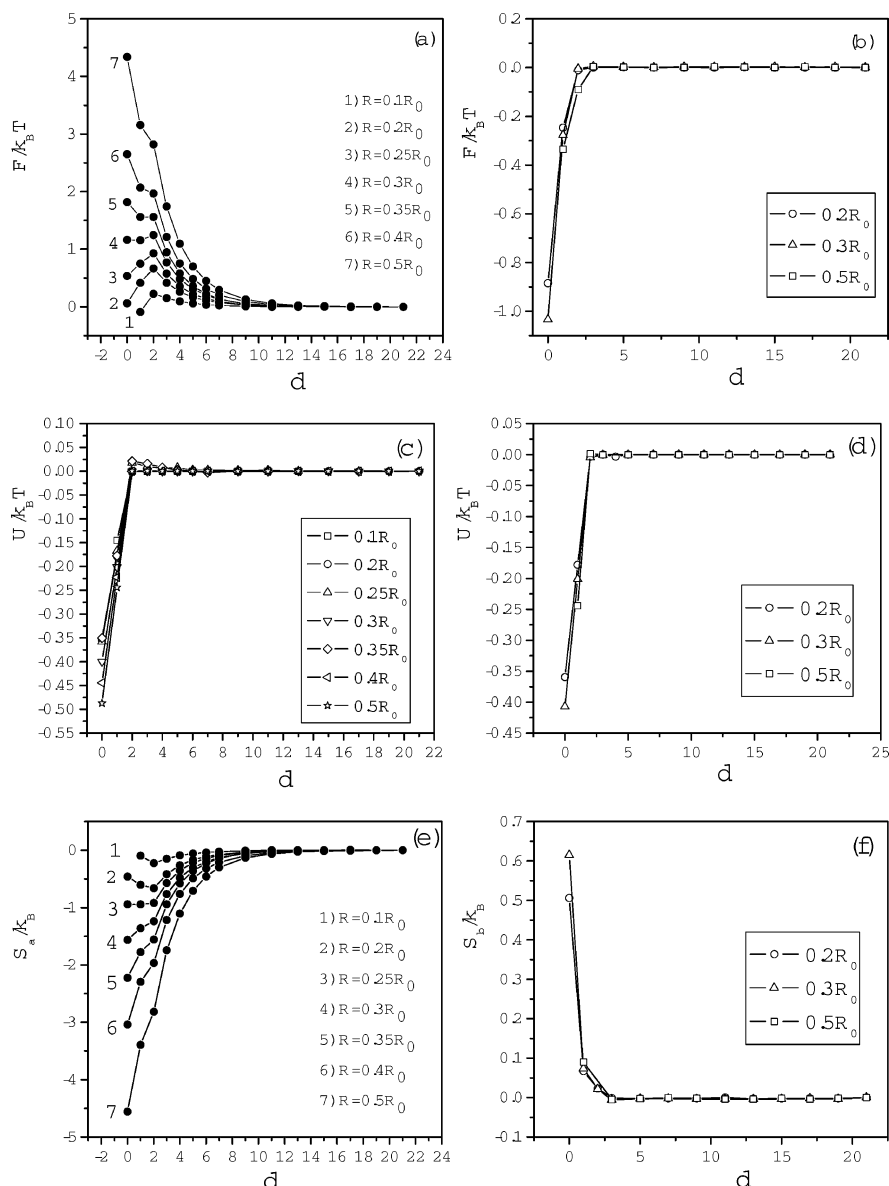*J. Phys. Chem. B, Vol. 109, No. 37, 2005* **17619**

Figure 2. Comparison of the free energy in the present brush system (a) and in the pure polymer melt (b), the interfacial energy in the present brush system (c) and in the pure polymer melt (d), and the brush entropy in the present system (e) and the free chain entropy in the pure polymer melt (f).

resulting equations can be solved self-consistently, and here, we implement the combinatorial screening algorithm of Drolet and Fredrickson.[57,58] A periodical boundary condition for the x-direction is applied, while, for the z-direction, the region of z < 0 is forbidden and the region of $z > Z_{max}$ is treated as a bath of solvent. Z_{max} is fixed to be $80a$, and the lateral simulation box size $L_x = 100a$ is large enough to avoid any influence due to the presence of colloidal particles.

We first examine the interaction energy of two colloidal particles (of radius R) deeply immersed in polymer brushes with the particle radii smaller than or comparable to polymer coils. Figure 2a gives the free energy, F, as a function of the lateral separation, d, between two colloidal particles, where the radii, R, of the particles are chosen as $0.1R_0$, $0.2R_0$, $0.25R_0$, $0.3R_0$, $0.35R_0$, $0.4R_0$, and $0.5R_0$ (from the bottom to the top), and the depth, h, is fixed at $12.0a$ which is smaller than the pure brush height (around $25.0a$). $R_0 \equiv aN^{1/2}$ characterizes the natural size of polymers, and we take $N = 100$ here. We find that, with increasing colloidal particle radius, the free energy curves change from shapes of short-range attraction and long-range repulsion into a purely repulsive one. The energy barrier height

is compared to the thermal energy, k_BT, and the position of the peak shifts from $d = 2.0\Delta$ to $d = 0$. In contrast, the position of the global minimum of free energy shifts to larger values of d, indicating a transition of favorite colloidal aggregation to colloidal dispersion. We also find that a weak double-peak behavior at middle particle sizes may exist (around $0.3R_0 \sim 0.35R_0$), where a local minimum is located at $d = 1.0\Delta$ and two peaks are located at $d = 0$ and 2.0Δ. For larger particles, the free energy decreases with d, but at $d = 2.0\Delta$, an inflection point still exists. For comparison, we calculate the free energy curves of corresponding particles in pure polymer melts instead of polymer brushes (see Figure 2b). On the contrary, we can see that, in polymer melts, the pair potential between colloidal particles is monotonically attractive despite the different sizes and the short-range interaction (about 2.0Δ) with distance.

To highlight the free energy feature shown in Figure 2a, we examine the free energy, F, of the colloidal particles in polymer brushes which is composed of three main contributions: interfacial energy between colloidal particles and polymer chains, entropy contribution due to space overlap of depletion zones (depletion potential), and entropic elastic stretching energy
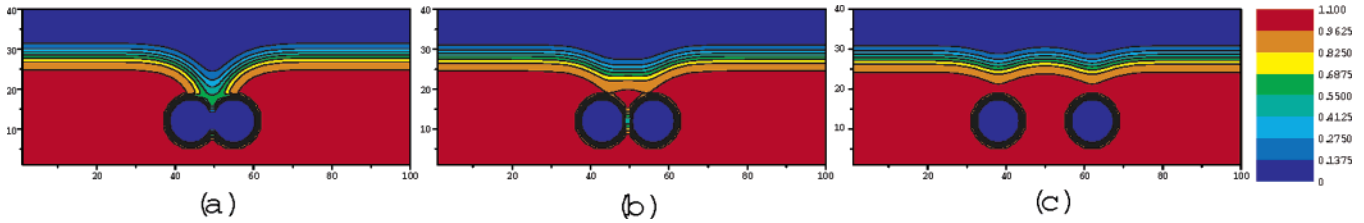
Figure 3. Concentration distributions of brush chains due to the presence of two colloidal particles with size $R = 0.5R_0$ and depth $h = 12.0a$: (a) $d = 0$; (b) $d = 2.0\Delta$; (c) $d = 13.0\Delta$.
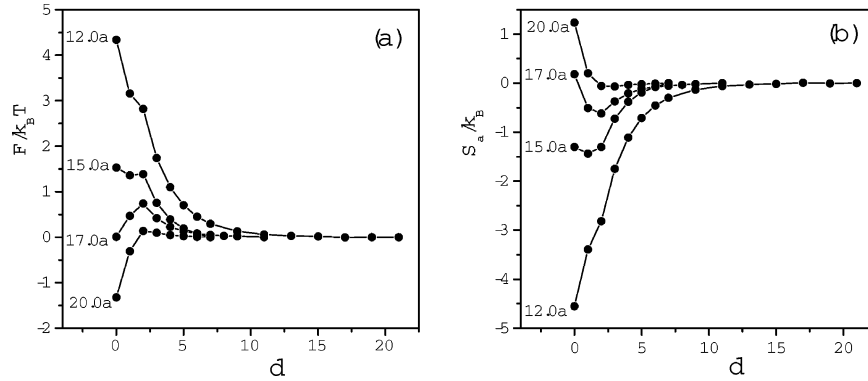

Figure 4. Free energy (a) and brush entropy (b) curves of the system when two particles of size $R = 0.5R_0$ are located in different penetration depths.

of brush chains due to the compression of particles. The interfacial energy is the same for the particles immersed in polymer brushes (Figure 2c) and in free polymer melts (Figure 2d) due to the same chemical nature of grafted and free chains. The interfacial energy curves exhibit a turning point at $d = 2.0\Delta$ because the depletion zones surrounding the two particles will overlap when the distance, d, is smaller than 2.0Δ, which will decrease the total interfacial area between colloidal particles and polymer chains. Figure 2f shows the entropy curves of free polymer chains when the colloidal particles are immersed in polymer melts. The free chain entropy change with the two-particle separation, d, mainly arises from the space overlap effect of depletion zones. When $d \leq 2.0\Delta$, two colloidal particles approach each other, and their depletion zones begin to overlap. This will increase the total volume accessible to the free polymer chains, leading to the increase of their entropy. Notice that, in Figure 2f, slight decreases of the entropy appear for $d \geq 2.0 \Delta$, and the entropy curves reach their minimum at $d = 3.0\Delta$. Such a behavior is due to the decrease of the conformational entropy of polymer chains confined between the two particle surfaces, because when d arrives at 3.0Δ the free polymer chain begins to be permitted through the region between the two particle surfaces. When the colloidal particles are immersed in polymer brushes, the entropy of grafted chains will include both the contributions of the space depletion effect and the entropic elastic effect of brushes (see Figure 2e). On one hand, the entropy due to chain compression reaches a minimum at zero distance ($d = 0$) and increases with the distance, d. The reason is that when the particles are far apart, the grafted chains will more easily fill the upper space through the interspace between the two particle surfaces to release the chain compression. Figure 3 shows the brush concentration distributions due to the presence of two colloidal particles for three different distances: $d = 0$, $d = 2.0\Delta$, and $d = 13.0\Delta$. The deformation of brushes is obviously weakened with an increasing separation of colloidal particles. On the other hand, the space depletion effect leads to the decrease of chain entropy with d for $d \leq 2.0\Delta$ where depletion zones surrounding the two particles overlap (see Figure 2f). It is the competition between the spatial depletion effect

around hard particles and the entropic elastic energy of brushes that leads to a possible appearance of the complex interaction for $0 \leq d \leq 2.0\Delta$ and the shift of minimum values of entropy curves from 2.0Δ to zero (Figure 2e). For small particles, the space depletion effect will dominate over the compression energy of brushes and the curve has a minimum at 2.0Δ. On the contrary, for large particles, the compression effect of brushes will become more important and determines the minimum point at $d = 0$. It is actually interesting that the brushes have a large entropic restoring force which easily controls the dispersions of colloids, in contrast to nonadsorbing polymer solvent. By comparing parts a and e of Figure 2, we find that the change of free energy is almost attributed to the entropic effect of brushes. On the other hand, we see from Figure 2c that the interfacial energy mainly enhances the formation of an inflection point at $d = 2.0\Delta$ and may lead to the onset of double peaks of the free energy curves for middle particle sizes.

To understand the brush entropy effects on effective interactions between two colloidal particles, we now consider the influence of the colloidal penetrating depth, h, on the free energy of the system for a fixed radius of colloidal particles. Parts a and b of Figure 4 give the free energy and brush entropy curves, respectively, for the particle size $R = 0.5R_0$ with depths of $h = 20.0a$, $17.0a$, $15.0a$, and $12.0a$. We can find that similar changes of curve shapes for different h values occur with the increase of d. At high h, the entropic compression energy of brush chains is small compared with the space depletion contributions. The free energy has a minimum value at $d = 0$ where the brush entropy reaches its maximum. As h is small, the compression contribution of brushes becomes dominant, and the minimum value of free energy tends to shift to a large separation of the particles. Correspondingly, the minimum point of the brush entropy moves from 2.0Δ to zero (Figure 4b). In particular, for middle depths where the spatial depletion effect of hard particles in polymer solution may compete with the entropic elastic energy of brushes, the richer interaction potentials such as repulsive barrier or double peaks may appear for free energy curves.
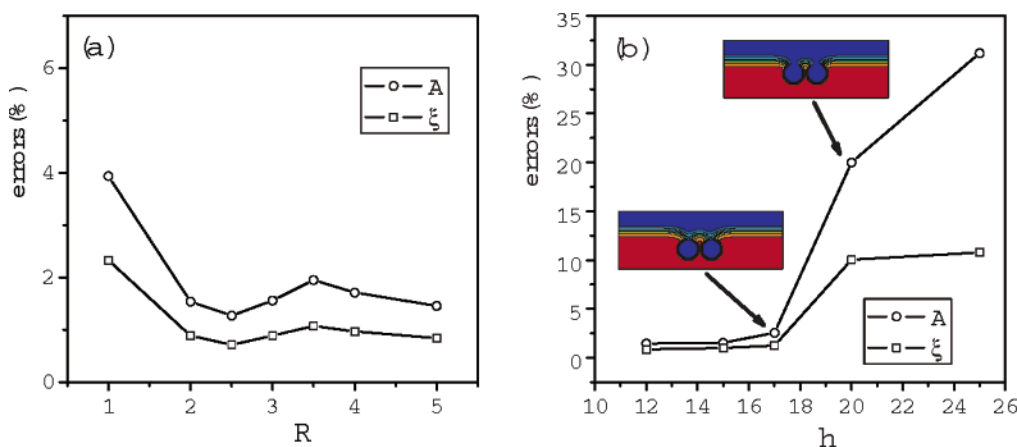
Interactions between Colloidal Particles

J. Phys. Chem. B, Vol. 109, No. 37, 2005 **17621**

Figure 5. Exponential-decay function fitting errors for amplitude, *A*, and decay length, ξ: (a) errors for two colloidal particles of different sizes immersed in a polymer brush; (b) errors for two colloidal particles of size $R = 0.5R_0$ under different penetrating depths, *h*.

To further examine the long-range force features due to the entropic elastic effect of brushes, finally, we define an exponential-decay function of free energy as $C_0 + A \exp(-d/\xi)$ with an increase in the two-particle separation, *d*. Figure 5 shows the fitting errors in percentage for the amplitude, *A*, and the decay length, ξ, as functions of colloidal particle size and colloidal penetrating depth, *h*, respectively. We find from Figure 5a that when colloidal particles are immersed in brushes, the errors are very small despite the different particle sizes. This means that the long-range particle−particle interaction mediated by polymer brushes has an excellent exponential-decay repulsive tail. Figure 5b provides the corresponding exponential-decay fitting errors in percentage for the long-range behavior of free energy curves as a function of penetration depth, *h*. We see that the errors, which reflect the degree of agreement with the exponential-decay behavior, have a sharp transition between $h = 17.0a$ and $h = 20.0a$ where the particles start to reach the brush−solvent surface (see the inset of Figure 5b). The result further addresses the fact that the deformation of brushes drives the occurrence of the exponential decay of long-range repulsions.

In summary, we have revealed a complex interaction between colloidal particles mediated by polymer brushes. Under different colloidal sizes and penetrating depths, we obtain complex attractive and repulsive interaction behaviors as a function of colloidal particle separation, due to the complex interplay among the entropic stretching energy of grafted polymers, entropic effects due to depletion zone overlap of hard particles, and the particle−polymer interfacial energy. The short-range attraction is mainly attributed to depletion effects of particles in polymer solutions, whereas the long-range interaction between penetrating particles is found to be a typical result of the brush entropy effect, which has a well-fitted exponential-decay repulsive tail. By simply using the grafting substrate, the present result indicates a possibility for governing the tendency of colloidal particles to flocculate into multiparticle aggregates or to remain dispersed and may have important implications for industrial processes, especially for biological systems.

Finally, we should stress that, in the present case, dimensionality is also an important factor. Here, the two-dimensional results can be effectively used to describe the interaction between two parallel long colloidal rods in three-dimensional experiment systems. However, for the case of colloidal spheres in three-dimensional systems, the deformation of grafted chains would be weakened (or larger colloidal spheres are needed to yield the equivalent deformation of grafted chains as in the two-dimensional case). Then, the peaks of the free energy curves (for example, in Figure 2a) are expected to decrease under the same parameters, and the transition between attractive and repulsive interactions will finally happen at a larger colloidal radius. Additionally, we also point out that the free energy difference caused by liquid and solid brushes will greatly depend on the grafting density of brushes. For low grafting densities, the chains of liquid brushes can easily relieve the deformation imposed by the colloidal particles by moving out of the region between colloids, which favors the effective attraction between colloidal particles at short distances. On the contrary, for the solid brush case where the ends of the chains cannot move away and the grafting density stays uniform, the total free energy and brush entropy will depend on the relative lateral positions between the colloidal particles and the grafting end points of chains on the substrate. For example, the existence of an immobile grafting chain between the colloidal particles will enhance the entropy repulsive barrier to particle−particle interaction at short distances. This means that the resulting curves of free energy and brush entropy obtained for mobile and immobile grafted chains will be obviously different. However, at high grafting density, even the mobile grafted chains cannot move easily due to the incompressibility constraint; that is, the grafting density almost stays uniform on the substrate for mobile grafted chains. On the other hand, the brush height increases with increasing grafting density, and thus, the grafted end effect on particles becomes less important. In this case, there is no distinct difference between liquid and solid brushes and the resulting free energy curves will be similar.

References and Notes

(1) Alivisatos, A. P. *Science* **1996**, *271*, 933.
(2) Godovski, D. Y. *Adv. Pol. Sci.* **1995**, *119*, 79.
(3) Whitesides, G. W.; Boncheva, M. *Proc. Natl. Acad. Sci. U.S.A.* **2002**, *99*, 4769.
(4) Russel, W. B. *Nature* **2003**, *421*, 490.
(5) Yethiraj, A.; van Blaaderen, A. *Nature* **2003**, *421*, 513.
(6) Gage, R. A.; Currie, E. P. K.; Stuart, M. A. C. *Macromolecules* **2001**, *34*, 5078.
(7) Liu, Z.; Pappacena, K.; Cerise, J.; Kim, J.; Durning, C. J.; O'Shaughnessy, B.; Levicky, R. *Nano Lett.* **2002**, *2*, 219.
(8) Bhat, R. R.; Genzer, J.; Chaney, B. N.; Sugg, H. W.; Liebmann-Vinson, A. *Nanotechnology* **2003**, *14*, 1145.
(9) Bhat, R. R.; Tomlinson, M. R.; Genzer, J. *Macromol. Rapid Commun.* **2004**, *25*, 270.
(10) Lopes, W. A.; Jaeger, H. M. *Nature* **2001**, *414*, 735.
(11) Thompson, R. B.; Ginzburg, V. V.; Matsen, M. W.; Balazs, A. C. *Science* **2001**, *292*, 2469.

(12) Thompson, R. B.; Ginzburg, V. V.; Matsen, M. W.; Balazs, A. C. *Macromolecules* **2002**, *35*, 1060.

(13) Lin, K. H.; Crocker, J. C.; Prasad, V.; Schofield, A.; Weitz, D. A.; Lubensky, T. C.; Yodh, A. G. *Phys. Rev. Lett.* **2000**, *85*, 1770.

(14) Heni, M.; Lowen, H. *Phys. Rev. Lett.* **2000**, *85*, 3668.

(15) Asakura, S.; Oosawa, F. *J. Chem. Phys.* **1954**, *22*, 1255.

(16) Tuinier, R.; Rieger, J.; de Kruif, C. G. *Adv. Colloid Interface Sci.* **2003**, *103*, 1.

(17) Rudhardt, D.; Bechinger, C.; Leiderer, P. *Phys. Rev. Lett.* **1998**, *81*, 1330.

(18) Sear, R. P. *Phys. Rev. Lett.* **2001**, *86*, 4696.

(19) Ilett, S. M.; Orrock, A.; Poon, W. C. K.; Pusey, P. N. *Phys. Rev. E* **1995**, *51*, 1344.

(20) Bolhuis, P. G.; Meijer, E. J.; Louis, A. A. *Phys. Rev. Lett.* **2003**, *90*, 068304.

(21) Verma, R.; Crocker, J. C.; Lubensky, T. C.; Yodh, A. G. *Phys. Rev. Lett.* **1998**, *81*, 4004.

(22) Guzman, O.; Kim, E. B.; Grollau, S.; Abbott, N. L.; de Pablo, J. J. *Phys. Rev. Lett.* **2003**, *91*, 235507.

(23) Kim, E. B.; Guzman, O.; Grollau, S.; Abbott, N. L.; de Pablo, J. J. *J. Chem. Phys.* **2004**, *121*, 1949.

(24) Mao, Y.; Cates, M. E.; Lekkerkerker, H. N. W. *J. Chem. Phys.* **1997**, *106*, 3721.

(25) Helden, L.; Roth, R.; Koenderink, G. H.; Leiderer, P.; Bechinger, C. *Phys. Rev. Lett.* **2003**, *90*, 048301.

(26) Mao, Y.; Cates, M. E.; Lekkerkerker, H. N. W. *Phys. Rev. Lett.* **1995**, *75*, 4548.

(27) Helden, L.; Koenderink, G. H.; Leiderer, P.; Bechinger, C. *Langmuir* **2004**, *20*, 5662.

(28) Oversteegen, S. M.; Wijnhoven, J.; Vonk, C.; Lekkerkerker, H. N. W. *J. Phys. Chem. B* **2004**, *108*, 18158.

(29) Han, Y.; Grier, D. G. *Phys. Rev. Lett.* **2003**, *91*, 038302.

(30) Crocker, J. C.; Grier, D. G. *Phys. Rev. Lett.* **1996**, *77*, 1897.

(31) Roth, R.; Evans, R.; Dietrich, S. *Phys. Rev. E* **2000**, *62*, 5360.

(32) Dijkstra, M.; van Roij, R.; Evans, R. *Phys. Rev. Lett* **1999**, *82*, 117.

(33) Louis, A. A.; Finken, R.; Hansen, J. P. *Phys. Rev. E* **2000**, *61*, R1028.

(34) Reister, E.; Fredrickson, G. H. *Macromolecules* **2004**, *37*, 4718.

(35) Roan, J.; Kawakatsu, T. *J. Chem. Phys.* **2002**, *116*, 7283.

(36) Roan, J.; Kawakatsu, T. *J. Chem. Phys.* **2002**, *116*, 7295.

(37) Solis, F. J.; Tang, H. *Macromolecules* **1996**, *29*, 7953.

(38) Satulovsky, J.; Carignano, M. A.; Szleifer, I. *Proc. Natl. Acad. Sci. U.S.A.* **2000**, *97*, 9037.

(39) Currie, E. P. K.; Norde, W.; Stuart, M. A. C. *Adv. Colloid Interface Sci.* **2003**, *100*, 205.

(40) Subramanian, G.; Williams, D. R. M.; Pincus, P. A. *Macromolecules* **1996**, *29*, 4045.

(41) Kim, J. U.; O'Shaughnessy, B. *Phys. Rev. Lett.* **2002**, *89*, 238301.

(42) Steels, B. M.; Leermakers, F. A. M.; Haynes, C. A. *J. Chromatogr., B* **2000**, *743*, 31.

(43) Steels, B. M.; Koska, J.; Haynes, C. A. *J. Chromatogr., B* **2000**, *743*, 41.

(44) For simplicity, here, we adopted a two-dimensional model; namely, the colloidal particles can be taken as two circles. However, the present model is easily extended to the three-dimensional case where the colloidal particles can take spherical or other shapes.

(45) Ferreira, P. G.; Ajdari, A.; and Leibler, L. *Macromolecules* **1998**, *31*, 3994.

(46) Matsen, M. W. *J. Chem. Phys.* **1997**, *106*, 7781.

(47) In ref 46, Matsen use a simple equation (eq 2) to describe the depletion interaction; however, the work focused on the morphologies of copolymers confined between two fixed plates (i.e., the effective interaction between two plates due to the existence of copolymers between them is not considered). In contrast, here the depletion zone is introduced to emphasize the study of depletion interaction between free colloids arising from surrounding polymer chains. For the same reason, the details regarding the segment profile at the two surfaces are not important, and thus, we will choose a similar form by Matsen (ref 46).

(48) We also calculated larger Δ values of the depletion zone and found that the physical features are qualitatively the same except for the small shifts of the peak of free energy curves.

(49) Lee, J. Y.; Shou, Z.; Balazs, A. C. *Phys. Rev. Lett.* **2003**, *91*, 136103.

(50) Schmid, F. *J. Phys.: Condens. Matter* **1998**, *10*, 8105.

(51) Matsen, M. W.; Schick, M. *Phys. Rev. Lett.* **1994**, *72*, 2660.

(52) Petera, D.; Muthukumar, M. *J. Chem. Phys.* **1998**, *109*, 5101.

(53) Matsen, M. W.; Bates, F. S. *J. Chem. Phys.* **1997**, *106*, 2436.

(54) Maniadis, P.; Thompson, R. B.; Rasmussen, K.; Lookman, T. *Phys. Rev. E* **2004**, *69*, 031801.

(55) Muller, M. *Phys. Rev. E* **2002**, *65*, 030802.

(56) Geisinger, T.; Muller, M.; Binder, K. *J. Chem. Phys.* **1999**, *111*, 5241.

(57) Drolet, F.; Fredrickson, G. H. *Phys. Rev. Lett.* **1999**, *83*, 4317.

(58) Drolet, F.; Fredrickson, G. H. *Macromolecules* **2001**, *34*, 5317.